Journal of Power Sources 205 (2012) 10–23

Contents lists available at SciVerse ScienceDirect

Journal of Power Sources

journal homepage: www.elsevier.com/locate/jpowsour

Review

A review on performance degradation of proton exchange membrane fuel cells during startup and shutdown processes: Causes, consequences, and mitigation strategies

Yi Yu [a,b], Hui Li [a,*], Haijiang Wang [a,**], Xiao-Zi Yuan [a], Guangjin Wang [b], Mu Pan [b]

[a] Institute for Fuel Cell Innovation, National Research Council Canada, 4250 Wesbrook Mall, Vancouver, BC, Canada V6T 1W5
[b] State Key Laboratory of Advanced Technology for Materials Synthesis and Processing, Wuhan University of Technology, Wuhan 430070, PR China

ARTICLE INFO

Article history:
Received 5 November 2011
Received in revised form 4 January 2012
Accepted 5 January 2012
Available online 20 January 2012

Keywords:
Proton exchange membrane fuel cell
Startup and shutdown process
Hydrogen/air interface
Reverse current
System strategies

ABSTRACT

Performance degradation during startup and shutdown is considered an important issue affecting the durability and lifetime of proton exchange membrane fuel cells (PEMFCs). Due to the high potentials experienced by the cathode during startup and shutdown, the conventional carbon support for the cathode catalyst is prone to oxidation by reacting with oxygen or water. This paper presents an overview of the causes and consequences of performance degradation after frequent startup–shutdown cycles. Mitigation strategies are also summarized, including the use of novel catalyst supports and the application of system strategies to prevent performance degradation in PEMFCs. It is found from the literature review that improvements in catalyst supports to prevent oxidation come at the expense of high cost, and the novel supports developed to date are not sufficient to completely prevent carbon oxidation in fuel cell engines. System strategies, including potential control and reaction gas control, have been developed and applied in fuel cell engines to alleviate or even avoid performance decay. This review aims to provide a clear understanding of the mechanisms related to degradation behaviors during the startup and shutdown processes, thereby helping fuel cell material or system developers in their efforts to prevent performance degradation and prolong the lifetime of PEMFCs.

Crown Copyright © 2012 Published by Elsevier B.V. All rights reserved.

Contents

* Corresponding author. Tel.: +1 604 221 3000.
** Corresponding author. Tel.: +1 604 221 3038.
E-mail addresses: hui.li@nrc.gc.ca (H. Li), haijiang.wang@nrc.gc.ca (H. Wang).

0378-7753/$ – see front matter. Crown Copyright © 2012 Published by Elsevier B.V. All rights reserved.
doi:10.1016/j.jpowsour.2012.01.059

1. Introduction

A fuel cell is an electrochemical device that can directly convert hydrogen energy to electricity. Among the various types of fuel cell, the proton exchange membrane fuel cell (PEMFC) is considered one of the most promising clean energy sources of the twenty-first century for transportation and stationary applications, due to its high energy conversion efficiency and power density, fast startup, and low/zero emission level [1,2]. Considerable research over the past few decades has significantly advanced PEMFC technology. However, some technological "bottlenecks" have limited its further commercialization. For example, the relatively short lifetime of PEMFCs, induced by materials degradation, is still unsatisfactory for stationary and automotive applications. The U.S. Department of Energy (DOE) lifetime targets for 2015 are 5000 h for transportation power systems and 40,000 h for stationary power systems [3], but current PEMFC technology yields only 1700 h and 10,000 h, respectively [4]. Insufficient fuel cell system durability is caused by degradation of the fuel cell components. The durability of each component in a PEMFC is affected by many internal and external factors, including material properties, fuel cell operating conditions (such as humidification, temperature, cell voltage, etc.), impurities or contaminants in the feeds, environmental conditions (e.g., subfreezing or cold start), operation modes (such as startup, shutdown, potential cycling, etc.), and the design of the components and the stack.

For automobile applications, PEMFCs must operate under various conditions, such as load changing cycles, high power conditions, idling conditions, and startup and shutdown cycles. Among these various dynamic conditions, startup and shutdown processes present a unique challenge for PEMFC systems, as they cause the cathode potential to become abnormally high, at which point the catalyst support is prone to be oxidized, resulting in adverse effects for fuel cell durability. Pei et al. investigated the durability of a PEMFC and evaluated its lifetime under startup and shutdown conditions [5]. The results suggested that performance decay under frequent startup and shutdown cycles is very serious, but the effect of startup and shutdown cycles on fuel cell lifetime can be ignored if the stack voltage is promptly dispelled after the fuel cell stops operating. However, quickly and completely dispelling the stack voltage is not easy, due to residual gas in the flow field after shutdown.

The recent literature contains several review papers on PEM fuel cell durability/reliability issues. Wu et al. [6] published a comprehensive review on PEMFC degradation mechanisms and mitigation strategies, in which durability tests under steady state [7–17] and dynamic state [18–30] conditions were also briefly summarized. In addition, Wu et al. [6] also discussed the major failure modes and mitigation strategies of different components in PEMFCs. Borup et al. [2] published an important review paper contributed by 56 researchers from national laboratories and universities in the United States and Japan who participated in a PEMFC Durability Workshop funded by the United States Department of Energy (DOE). This review provided comprehensive discussions on fundamental and scientific aspects of PEMFC durability, such as operational effects on fuel cell durability, but its main focus was on the degradation of components, including the membrane, catalyst layer, and gas diffusion layer. Vahidi et al. [31] in their review introduced the main parameters influencing the long-term performance and durability of PEMFCs. Zhang et al. [32] provided a review of Pt-based catalyst layer degradation in PEMFCs, including a very detailed discussion of the carbon corrosion mechanisms under gross fuel starvation and the air/fuel boundary; mitigation strategies were also introduced, among them carbon support improvement and system strategies.

All these reviews have touched on performance degradation and carbon oxidation during the startup and shutdown cycles, but there is no comprehensive review of PEMFC durability studies and mitigation strategies under startup and shutdown conditions. Over the last few years, in an effort to enhance the lifetime of PEMFC systems for automobile applications undergoing frequent startup and shutdown, significant progress has been made in the development of novel catalyst supports. In addition, various system strategies for tackling startup and shutdown issues have been developed and reported through a considerable number of papers and patents. There is thus a need for a detailed review of degradation mechanisms and all known mitigation strategies, including materials improvement and system strategies for startup and shutdown processes, to help fuel cell material developers or fuel cell system developers in their efforts to prevent performance degradation and prolong the lifetime of PEMFCs for automotive applications.

The purpose of this review is therefore to summarize the studies conducted by academic and industrial researchers on the durability of PEMFCs during startup and shutdown. First, a description of startup and shutdown processes is provided for a clear understanding of what happens to fuel cells during these processes. Second, accelerated lifetime tests under startup–shutdown cycle conditions, conducted by both academic and industrial researchers, are summarized and discussed. In addition, the major failure modes and root causes of degradation during startup and shutdown processes are discussed in detail. The review concludes with a detailed introduction of recently developed mitigation strategies, including materials improvement and system strategies, based on an exhaustive survey of journal papers and patents.

2. Startup and shutdown processes

Both startup and shutdown are dynamic processes that a fuel cell inevitably must confront in automobile applications. Compared to steady-state processes, startup and shutdown processes experience different profiles under operating conditions. For example, the cell temperature, gas humidity, and local gas mixture are different than under steady-state conditions—for example, increasing temperature and humidity during startup, and decreasing temperature and humidity during shutdown. However, the major feature during startup and shutdown, a feature that is also the major cause of performance degradation during those processes, is the local gas mixture at the anode, which is commonly called the hydrogen/air interface or the fuel/air interface. To clearly understand the accelerated lifetime tests and degradation mechanisms associated with startup and shutdown processes, a brief introduction to these processes is given below and a schematic graph is presented in Fig. 2.

2.1. Startup process

The startup process for the fuel cells referred to in this paper excludes cold start below freezing temperatures. In the normal operation of fuel cell engines, air fills the anode flow field after

extended shutdown, due to permeation by atmospheric air from the anode exhaust or across the membrane. The first step of the startup process is to introduce air or oxygen into the cathode and hydrogen into the anode. Because of the presence of air in the anode, there is a hydrogen/air interface in the anode flow field during hydrogen introduction. As hydrogen is supplied continuously during the startup process, the air is dispelled from the anode inlet to the anode outlet, resulting in a floating hydrogen/air interface. The faster the hydrogen is supplied, the more briefly is this interface present. Eventually, all the air in the anode is dispelled by the hydrogen, and the air/hydrogen interface disappears, leading to the state of the open circuit voltage (OCV) for fuel cells. In a laboratory test, to prevent fuel cells from forming this hydrogen/air interface, the anode and cathode flow fields are purged with nitrogen to protect the fuel cells before the startup process. However, in the real operation of fuel cell engines, a nitrogen supply is not practical, resulting in an air/hydrogen interface during startup.

In addition, if the fuel cell experiences bad gas flow distribution during the startup process (called local fuel starvation), oxygen could cross the membrane from the cathode to the anode under a pressure or concentration gradient, resulting in a hydrogen/air interface.

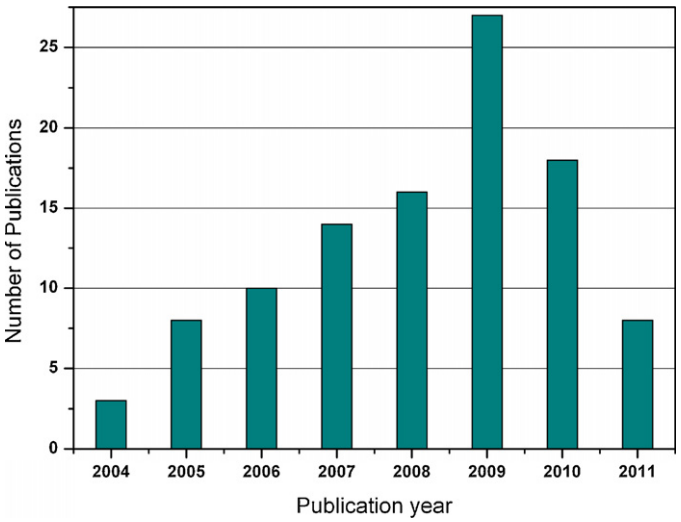

Fig. 1. Publication history of articles after 2004 on the startup and shutdown processes of PEMFCs.

2.2. Shutdown process

The same situation of a hydrogen/air interface can also occur in the shutdown process. When the primary load is shut off, the fuel cell's shutdown process begins. After the hydrogen and air supplies are shut off, residual gas will remain in the gas channels at the anode and cathode. Because of the gas concentration difference between the anode and cathode, the oxygen at the cathode crosses the membrane to the anode, resulting in a hydrogen/air interface at the anode. Moreover, after extended shutdown, atmospheric air will permeate the fuel cell from the anode outlet due to seal failure. The air/hydrogen interface will remain for a much longer time than when it is introduced directly via the hydrogen supply in the startup process, due to slow air permeation during shutdown.

To investigate the effect that the hydrogen/air interface has on the performance of PEM fuel cells during the startup and shutdown processes, many researchers have focused on accelerated lifetime tests under startup–shutdown cycle conditions in the laboratory.

3. Degradation of PEMFC during startup and shutdown

3.1. Accelerated lifetime tests under startup–shutdown cycles

In recent years, significant research efforts have been focused on degradation behaviors under startup and shutdown conditions, as indicated by the number of publications shown in Fig. 1. In these publications, most of the durability tests were conducted under accelerated conditions, due to the complexity and difficulty of mimicking and controlling startup and shutdown procedures. To conduct durability tests for startup and shutdown cycles, the hydrogen/air interface must be introduced at the anode, which demands high standards of test condition controls and safety controls in the laboratory. As a result, durability tests under startup and shutdown conditions are costly, as the requisite experiments are lengthy. Accelerated tests are therefore commonly used. United Technologies Corporation (UTC) and a group at the Fuel Cell Research Center, Korea Institute of Science and Technology, have conducted a considerable amount work on accelerated tests to investigate degradation mechanisms and develop system strategies for startup and shutdown processes.

As shown in Table 1, Cho et al. from the Fuel Cell Research Center at the Korea Institute of Science and Technology have investigated several operating parameters [33–39] that can have an impact on the degradation rate of PEMFCs under startup and shutdown cycles, including cathode humidity [37,38], cell temperature [33], application of a dummy load [35,36], and gas supply sequences [34]. The hydrogen/air interface during the startup and shutdown processes was mimicked by purging the anode and cathode channels with air after continuous air and hydrogen were supplied. During this purging process, the test conditions—including cell temperature, gas humidity, and gas supply sequences—were changed to investigate the resulting effects on the degradation behaviors of fuel cells. The results indicated that performance degradation was alleviated at lower humidity and lower cell temperature with the dummy load during startup and shutdown. Similarly, Lee et al. [39] also investigated the effect of the hydrogen/air interface on fuel cell performance degradation. In their study, the hydrogen/air interface was created by replacing hydrogen with air at the anode, to investigate carbon corrosion at the cathode. It was concluded that to prevent the degradation of PEMFCs caused by residual gases, hydrogen should be removed from the anode gas channel by air purging, which was found to be very effective.

Takagi et al. [40] investigated the effect that the shutoff sequence of hydrogen and air had on the fuel cell performance degradation rate. The startup and shutdown process was operated as follows: (1) hydrogen and air were supplied to the anode and cathode, respectively, and the cell was operated for 1–1.5 min under a constant load current. (2) The load current was turned off to maintain the OCV state, and simultaneously either the air or the hydrogen supply was shut off at that point. (3) When the cell voltage dropped to 0.2 V, the other gas supply was shut off. (4) After leaving the cell shut down for 5 min while maintaining the cell temperature at the same level as had been used during operation, both hydrogen and air were supplied simultaneously and the load current was applied again to operate the cell. It was concluded that in the interest of system safety and fuel efficiency, it would be more beneficial to shut off the hydrogen supply before the air supply. Nevertheless, to prevent performance degradation during the shutoff process, the air supply should be closed prior to the hydrogen supply to prevent air permeation to the anode, which would otherwise result in a hydrogen/air interface at the anode during the shutdown process. Inukai et al. [41] simulated startup/shutdown cycles by exchanging hydrogen and air at the anode. During this gas exchange, the distribution of oxygen partial pressures at the anode was visualized

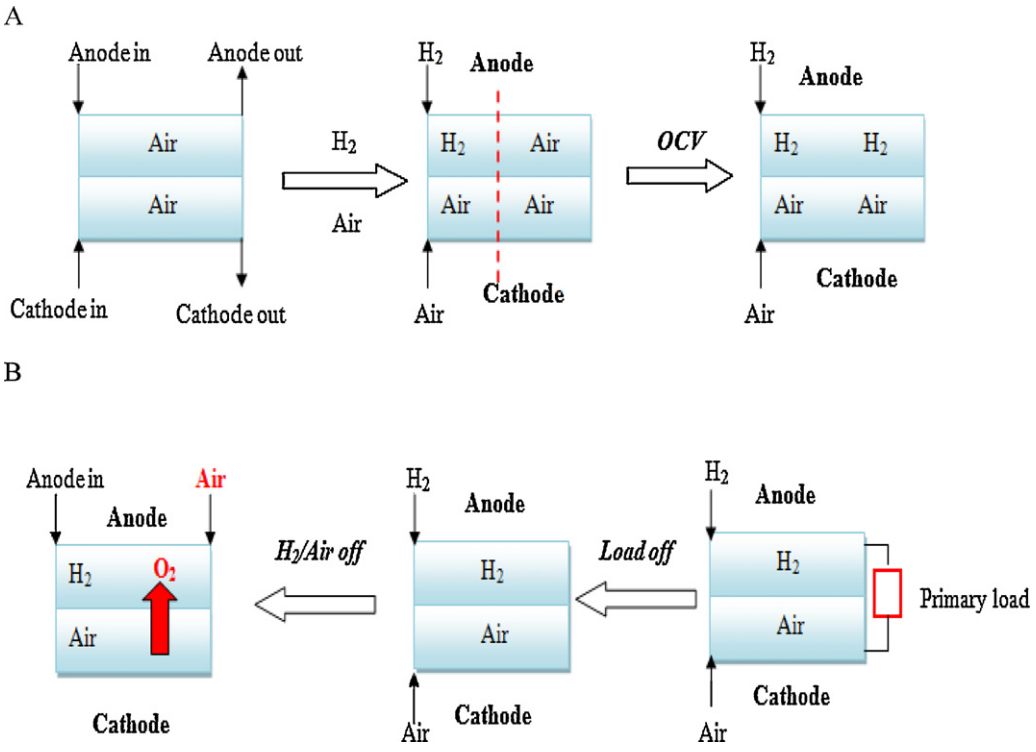

Fig. 2. Description of the startup (A) and shutdown (B) processes.

using a real-time/space visualization system, which clearly showed the location of H_2-rich and O_2-rich areas along the gas-flow channel from the inlet to the outlet. They observed that the gas exchange rate was much slower than what would be predicted from simple replacement, and that it correlated with the proton transfer derived from carbon corrosion of the cathode catalyst layer. From these visualization results they found that the shutdown process resulted in more serious effects than the startup process.

In addition to those studying the startup and shutdown processes by replacing hydrogen/air or exchanging gases to introduce the hydrogen/air interface at the anode, other research groups have studied the processes using a reformatted gas supplied to

Table 1
Summary of PEMFC durability tests under startup and shutdown cycles.

Authors	Experimental factors	Number of cycles	Degradation rate	Reference
Qi et al.	Air/fuel boundary	80	5 mV drop per cycle at 400 mA cm^{-2}	[42]
Darling et al.	Localized fuel starvation	100 h	Severe damage to the catalyst layer	[44]
Takagi et al.	Shutoff sequence of hydrogen and air without a dummy load	40	Output power declined by 17% at 1.0 A cm^{-2}	[40]
Pei et al.	Start-stop cycling with nitrogen purge	80 h	Cell voltage decayed by 0.00196% at 100 A per cycle with 280 cm^2 active area PEMFC stack	[5]
Owejan et al.	Graphitized carbon in MPL	25 h	63% loss in current density at 0.6 V without graphitized carbon, 25% improvement in voltage degradation at 1.2 A cm^{-2}	[30]
Lim et al.	Shutdown process	200	0.31 mV drop per cycle at 80 °C and 400 mA cm^{-2}	[35]
Sakamoto et al.			50–90 μV drop per cycle	[22]
Cho et al.	Air purging effect	50	4.2 mV drop per cycle with air/hydrogen purge 2.0 mV per cycle with air/air purge	[39]
	Applying the dummy load	1200	Cell voltage decayed by 0.030% with dummy load but by 0.068% without dummy load	[36]
	Cathode inlet relative humidity (RH)	1500	0.186 mA cm^{-2} drop per cycle for 0%RH 0.240 mA cm^{-2} drop per cycle for 50%RH 0.266 mA cm^{-2} drop per cycle for 100% RH	[37,38]
	Supply sequence of hydrogen and air	1200	0.68 mA cm^{-2} drop per cycle with concurrent air and hydrogen supply; 0.47 mA cm^{-2} per cycle with hydrogen supplied prior to air	[34]
	Fuel cell temperature	1200	0.13 mV drop per cycle at 40 °C 0.24 mV drop per cycle at 65 °C 0.31 mV drop per cycle at 80 °C at 400 mA cm^{-2}	[33]
Ettingshausen et al.	Start/stop cycling	500	About 0.66 mV drop per cycle at 1000 mA cm^{-2}	[45]
Yu et al.	Cathode exhaust condition	1500	0.024 mV drop per cycle for closed cell; 0.093 mV drop per cycle for open-ended cell at 1000 mA cm^{-2}	[43]
Inukai et al.	Gas exchange cycling	500	About 0.9 mV drop per cycle at 200 mA cm^{-2}	[41]
Knights et al.	Relative humidity on Ru dissolution and crossover			[46]

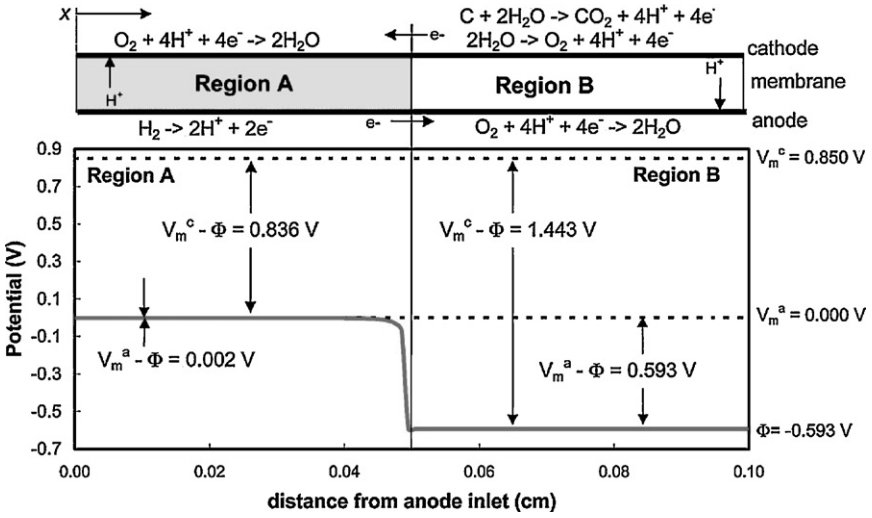

Fig. 3. Potential distribution along anode flow path during reverse-current conditions.
Reprinted with permission from Ref. [47]. Copyright 2005, The Electrochemical Society.

the anode, or using an open cathode exhaust end. Instead of pure hydrogen for the anode gas supply, Qi et al. [42] used a reformate gas composed of 10 ppm CO, 49% H_2, and 17% CO_2, balanced by N_2. A 2% air bleed was used at the anode side to mimic a hydrogen/air interface. The results indicated a degradation rate of about 5 mV per cycle at 400 mA cm^{-2} after 80 cycles. However, 10 ppm CO and 17% CO_2 in the reformatted gas also augmented the PEMFC degradation rate, which should not be ignored. Yi et al. [43] studied the effect of cathode exhaust conditions on the degradation behaviors of PEMFCs during the shutoff process. The hydrogen/air interface was simulated by using the open exhaust at the cathode to lead to atmospheric air permeation. They concluded that the closed cathode exhaust was beneficial for PEMFC durability.

The accelerated testing results discussed above not only demonstrate the adverse effects that startup and shutdown processes can have on the durability of a PEMFC, but also provide information on how to alleviate these adverse effects by changing operating conditions, such as humidity, temperature, etc. However, the condition changes mentioned in those papers are not practical for real fuel cell operation. For example, the performance degradation caused by startup and shutdown could be mitigated with lower temperatures and lower gas humidity during the startup and shutdown cycles. However, under real conditions it would be difficult to control the temperature and humidity before starting up or shutting down the system. Furthermore, it would take a long time to lower the temperature and humidity from their working points to their shutdown points. Another impractical tactic would be shutting off the air supply prior to the hydrogen supply; although this would mitigate the adverse effects of the startup and shutdown process, it is not advisable for either system safety or fuel efficiency. In addition, as shown in Table 1, although most tests conducted under optimized operating conditions and frequent cycles demonstrated some level of improvement in degradation rates, these improvements were still not enough to meet the DOE lifetime targets.

Hence, more practical and effective procedures should be developed to mitigate the performance degradation caused by startup and shutdown cycles. In Section 4.2, we explore in depth a few system strategies put forward by UTC that could be practically applied in real fuel cell systems and result in much better durability.

3.2. Root cause of PEMFC degradation during startup and shutdown

As discussed earlier, the hydrogen/air interface formed during the startup and shutdown processes is the root cause of the negative effects that these processes have on PEMFC durability. In this part we will discuss the underlying degradation mechanisms caused by the hydrogen/air interface in a PEMFC.

3.2.1. Reverse current

The reverse current mechanism was first proposed by UTC in 2005 [47]. As discussed in Section 2, they pointed out that a hydrogen/air interface in the anode was created during both the startup and shutdown processes. When this happens, as shown in Fig. 3, part of the anode is filled with hydrogen and the rest is filled with air, leading to a region where oxygen reduction occurs on both the cathode and anode sides, resulting in a high potential difference (about 1.44 V) at the cathode. This high cathode potential

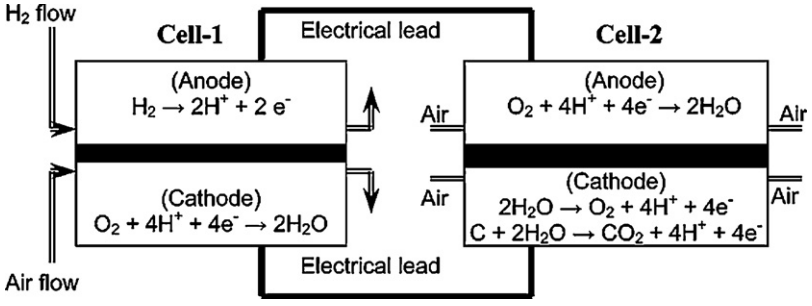

Fig. 4. Schematic of a dual cell configuration used to simulate the reverse-current condition.
Reprinted with permission from Ref. [47]. Copyright 2005, The Electrochemical Society.

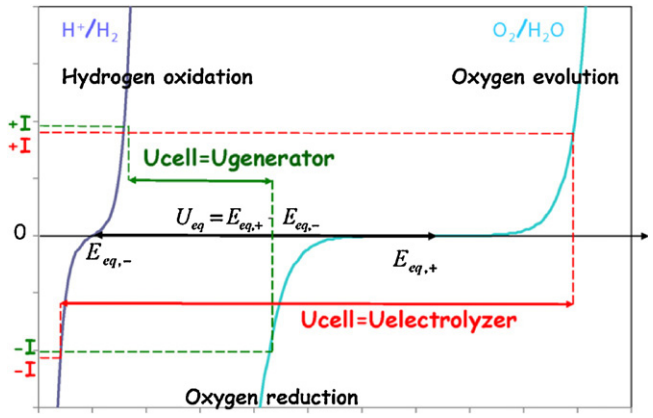

Fig. 5. Intensity potential curves for two electrodes of an electrochemical cell. Reprinted from Ref. [48] with permission.

temporarily reverses the current where air is present in the anode, causing severe carbon oxidation (also shown in Fig. 3). They proposed using high cathode potential and "reversed current", based on the significant decrease in the catalyst layer that they observed in a single-cell experiment. However, they did not directly measure the value of the high cathode potential; instead, they used a dual cell configuration to estimate the cathode voltage to be around 1.44 V. As shown in Fig. 4, in their dual cell configuration, the two single cells were connected by conductive wires, which would certainly lead to some voltage loss at the interface of the two single cells. However, under the real condition of a single cell, Cell 1 and Cell 2 in Fig. 4 would be connected by an electrolyte and an electrode, so the resistance between the two cells should be negligible. Therefore, the accuracy of their estimated 1.44 V cathode potential is debatable.

Based on the same premise of "reversed current" and high cathode potential, other groups also conducted similar analyses and tests. Yousfi-Steiner [48] explained the observed degradation at the cathode by heterogeneities in current distribution, with local current close to zero in the area fed with nitrogen or diluted oxygen. According to Yousfi-Steiner's assumption, since the two cells in this configuration are connected to neither an electronic load nor a potentiostat, and since they are only externally connected, the setup presented in Fig. 4 most likely represents a generator (Cell 1) connected in series to an electrolysis cell (Cell 2), rather than two single fuel cells connected in parallel [49]. Analyzing the current flow and calculating the voltage in the two devices yields the conclusion that the positive electrode of Cell 2 can reach high enough potentials for fast carbon and Pt corrosion to occur, as shown in the given formulas and Fig. 5.

Similarly, Owenjan et al. [30] have considered the PEMFC under the startup and shutdown cycles as two shorted cells. The section of the cell where air was present in both the anode and the cathode was considered an air/air cell, and the section where the cathode was filled with air and the anode was filled with hydrogen was considered a normal PEMFC. Their assumption was similar to Yousfi-Steiner's, but they did not predict or measure the value of the cathodic potential during the startup and shutdown processes.

Reverse current has become a commonly accepted mechanism to explain the degradation induced by the startup and shutdown processes. As a result, many research efforts have been directed to measuring or predicting the high potential at the cathode. The following paragraphs summarize the experimental measurements and model predictions of the cathode potential during startup and shutdown. Due to the instantaneous nature of the hydrogen/air interface at the anode, the occurrence of high potential at the cathode is also instantaneous, which presents great challenges for correctly measuring this potential. In recent papers, several methods have been reported to test the cathode potential:

- **Dual cell configuration**: Two single cells were connected externally by electric wires. The anode and the cathode of the first single cell were supplied with hydrogen and air, respectively, as in a normal PEMFC. In the other cell, air filled the anode and cathode to simulate an electrolysis cell or a driven cell [42,47,48]. The cathode potential of the second cell was the maximum cathode potential of a PEMFC exposed to reverse current. As discussed above, in the real condition of a single cell, Cells 1 and 2 would be connected by an electrolyte and an electrode, not external wires, which produced a voltage loss at the interface of the two single cells. A much smaller voltage loss would occur in a real situation. Consequently, some errors probably resulted from the external connection.
- **Reference electrode method**: Since it is not possible to distinguish between the anode and cathode half-cell reactions with a segmented fuel cell assembly, the reference electrode method has been developed and employed by several research groups [50–55]. Measurement of the cathode potential was achieved by introducing a constant potential into the test cell, utilizing a reference electrode, and then the anode and cathode potentials could be determined relative to this constant potential. In this method, a small strip of membrane in the MEA was soaked in sulfuric acid with a mercury sulfate reference electrode [50] or a hydrogen reference electrode [56]. Both the anode side and the cathode side of the MEA were considered the working electrode. The cathode potential could be measured as the potential difference between the working electrode and the reference electrode. However, it should be pointed out that the reference electrode method also has its drawbacks. Because the reference electrode is placed at a special point on the membrane, the potential measured at this particular point may not correctly reflect the real potential of the whole membrane. Therefore, it would be more accurate to develop a test device that can evaluate the potential of the whole membrane, rather than the potential of a special point on the membrane.
- **Model prediction**: To overcome the disadvantages in the experimental measurements mentioned above, some researchers have developed mathematical models to obtain the electrolyte potential profile for this phenomenon [47,57,58]. The results can assist researchers in clearly understanding degradation mechanisms.

Table 2 summarizes the methods used to measure cathode potential during startup and shutdown, as reported in recent publications. The researchers at Plug Power measured the value of the cathodic potential with reformate hydrogen as the fuel [42]. By using a dual cell configuration, a cathode potential as high as 1.75 V was measured, which was different from the calculated value reported by Reiser et al. [47]. Baumgartner et al. [50] obtained a cathode electrode potential of up to 1.5 V with four reference electrodes under hydrogen starvation conditions, which also resulted in a H_2/air boundary in the anode. Shen et al. [56] measured the cathode, anode, and membrane potentials versus a hydrogen reference electrode using a special electrode design, as shown in Fig. 6; the results indicated that the interfacial potential difference between the cathode and the membrane was as high as about 1.6 V. All these experiments prove that high potential does exist at the cathode of a PEMFC during the startup and shutdown processes.

However, Sidik et al. [57] proposed a different view on the maximum potential a PEMFC cathode could experience due to the formation of a hydrogen/air interface at the anode. They clarified that the maximum potential was about twice the potential observed when one connected a driving fuel cell to a driven cell, based on the Butler–Volmer equation and the experimental data

Table 2
Summary of the cathode potential measurements or predictions for the startup and shutdown processes, as reported in recent publications.

Authors	Test methods	Cathode potential value	Reference
Qi et al.	Dual cell configuration	1.75 V	[42]
Reiser et al.	Model prediction	1.44 V	[47]
Baumgartner et al.	Four reference electrodes	1.5 V	[50]
Shen et al.	Hydrogen reference electrode	1.6 V	[56]
Tak et al.	Dynamic hydrogen electrode (DHE)	1.4 V	[59]
Sidik et al.	Theoretic analysis	Twice the OCV of the driving cell	[57]
Ohs et al.	Modeling study	>1.2 V	[58]

from PEMFCs (In Fig. 3, the driving cell is Cell 1 and the driven cell is Cell 2.). Because of some simplifications employed in Reiser's model, the predicted cathode potential was 1.44 V, which was lower than twice the OCV.

It can be concluded from the measured or predicted cathode potentials discussed above that, in spite of the different methods, the maximum potential value at the cathode is much higher than the OCV. At such a high potential, the carbon support of a Pt-based catalyst is prone to oxidation, resulting in PEMFC performance degradation.

In addition to measuring or mathematically predicting the high cathode potential experienced during the startup and shutdown processes, researchers have also conducted other related tests, such as measuring the current distribution in segmented cells [60–62], monitoring the concentration of CO or CO_2 during startup and shutdown [59,63], evaluating the effect of cell design (flow field structure and GDL thickness) on start–stop phenomena [64,65], and conducting modeling studies [58,66–73] on water management and carbon-corrosion during startup and shutdown. All the test results have confirmed performance degradation during the startup and shutdown processes of PEMFCs.

3.2.2. Fuel starvation

Localized fuel starvation can happen during normal operation due to poor distribution of reactants or to water flooding. However, during unprotected fuel cell startup and shutdown, a hydrogen/air boundary forms, which in some cases leads to a situation similar to fuel starvation. This section discusses in a general way the consequences that fuel starvation can have on fuel cell performance and durability. But it has to be pointed out that fuel starvation is not limited to startup and shutdown.

In the normal operation of PEMFCs, all the reactants are sufficiently supplied to the anode and the cathode, resulting in even distribution at the electrode surface. However, if heterogeneous fuel distribution occurs, air or oxygen at the cathode will cross the membrane to the anode, due to the pressure difference between the anode and cathode. In 2008, Ofstad [74] reported creating a transient hydrogen/air interface in the anode layer. In Jingwei's modeling study [73], the results indicated that the rate of carbon corrosion at the cathode side of the fuel starvation region was strongly dependent on oxygen diffusion through the membrane. The concentration gradient across the membrane is the driving force for oxygen to permeate from the cathode to the anode, according to Fick's first law. If we suppose a fuel cell system in a steady state, the concentration of oxygen remains constant at all surfaces of the membrane [75]. Under this assumption, the one-dimensional diffusion equation from Fick's first law is expressed as [76]:

$$J_{O_2} = -D_{O_2}\frac{dC_{O_2}}{dz} = D_{O_2}\frac{C_{O_2}^{\text{cathode}} - C_{O_2}^{\text{anode}}}{z} \quad (1)$$

where J_{O_2} is the oxygen permeation rate, D_{O_2} is the oxygen diffusion coefficient, $C_{O_2}^{\text{cathode}}$ and $C_{O_2}^{\text{anode}}$ are the respective oxygen concentrations on the surface of the membrane at the cathode and anode, and z is the membrane thickness. As a result, a hydrogen/air interface is produced at the anode. According to the "reverse-current mechanism" [47], this interface is not beneficial to the durability of the carbon support in PEMFCs.

Some researchers have investigated the current distribution of PEMFCs during local fuel starvation [50,77–83], and Yousfi-Steiner et al. [48] provided an excellent review of the causes and consequences of starvation issues. So in this review, we will turn from performance degradation due to local fuel starvation arising from a hydrogen/air interface, and focus in Section 4 on materials improvement and system strategies to mitigate catalyst decay during the startup and shutdown processes.

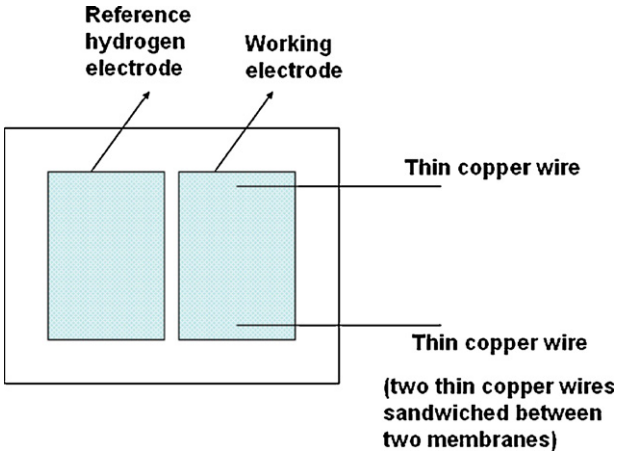

Fig. 6. Schematics of test MEA with reference hydrogen electrode and thin copper wires sandwiched between two membrane.
Reprinted from Ref. [56] with permission.

3.2.3. Carbon oxidation

Catalyst degradation at the cathode is considered a major failure mode for PEMFCs when the catalysts are exposed to reverse-current conditions during startup and shutdown.

In the catalyst layers of PEMFCs, platinum nanoparticles are always dispersed on supports to increase the active area and thereby lower material costs [84–86]. As concluded in Ref. [87], the ideal catalyst support should have the following properties:

- Reasonably high electrical and thermal conductivity.
- Good corrosion resistance in the electrolyte.
- Dimensional and mechanical stability with reasonable strength.
- High surface area.
- Availability at low cost and with reasonably high purity.
- Easy dispersion of small catalyst particles.
- Easy fabrication into electrodes.
- Absence of adverse corrosion products.

Because of its good electronic conductivity and low cost, carbon is widely used as a fuel cell catalyst support. Although carbon has most of the above properties, it is susceptible to oxidation or

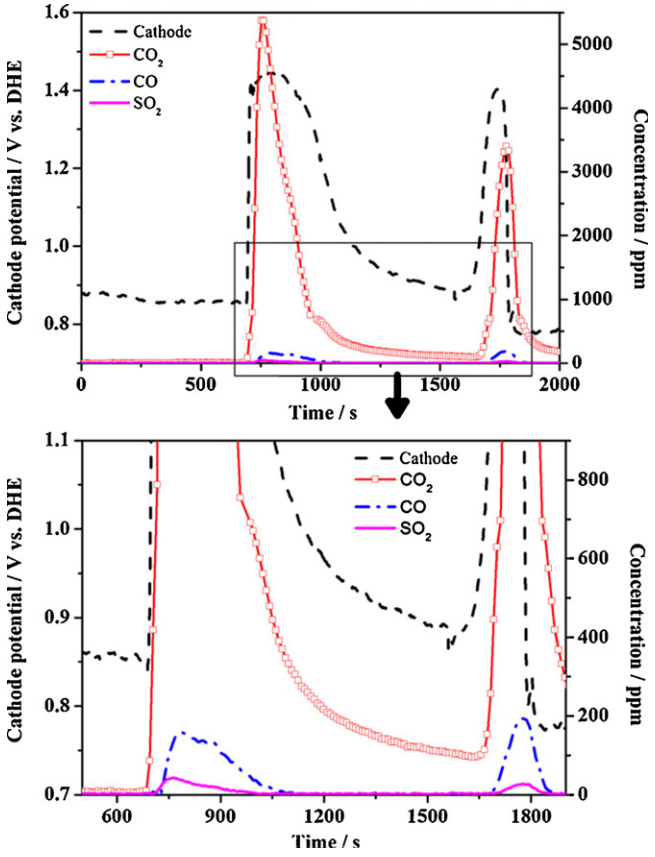

Fig. 7. Quantitative analysis of cathode outlet gases with change in cathode potential.
Reprinted from Ref. [59] with permission.

corrosion at high temperature and high oxygen concentration, yielding CO_2 or CO, as in the following equations [42,63]:

$$C + 2H_2O \rightarrow CO_2 + 4H^+ + 4e^- \quad (2)$$

$$C + H_2O \rightarrow CO + 2H^+ + 2e^- \quad (3)$$

Shao et al. [88] investigated the thermodynamic potential of carbon oxidation into CO_2. Their results indicated that once the potential was higher than +0.207 V vs. RHE, the carbon would be oxidized to CO_2, according to reaction (2). Carbon can also be oxidized to CO at 0.518 V under standard conditions [63,89,90].

In normal fuel cell operation, the carbon oxidation rate is slow due to the slow kinetics of reactions (2) and (3) at PEMFC operating temperatures. However, carbon oxidation occurs much faster under dynamic processes such as startup and shutdown, because the cathode potential is much higher than the thermodynamic potential of carbon oxidation. It has been reported that although the kinetics of the carbon oxidation reaction is sluggish at low potential and low temperature, the presence of Pt particles will accelerate carbon oxidation [90]. Kim et al. [59] directly measured and analyzed exhaust gas using FT-IR during start/stop operation. As shown in Fig. 7, the amount of CO_2 evolved was proportional to the cathode potential at values above 1.0 V. In addition, at potentials higher than 1.2 V, CO and SO_2 were generated, having detrimental effects on fuel cell performance. Similarly, S. Mass measured the CO_2 and CO concentrations in cathode exhaust using non-dispersive infrared spectroscopy (NDIR) [63]. More directly, Inukai et al. used scanning transmission electron microscopy (STEM) images to investigate catalyst-layer degradation at the cathode during 500 start/stop cycles. They observed several holes at the catalyst layer, with no

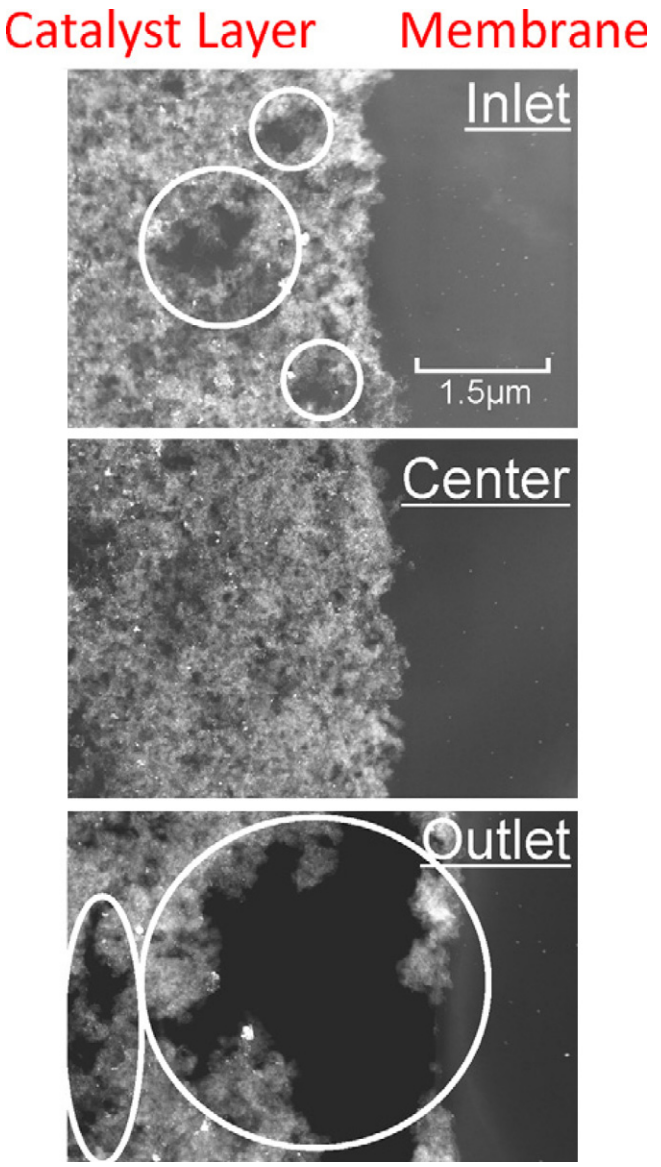

Fig. 8. STEM images near the inlet, center, and outlet of an MEA at the cathode after degradation.
Reprinted from Ref. [41] with permission.

carbon support, indicating a drastic corrosion of the carbon support [41] (Fig. 8).

Nano-particles such as Pt particles in the catalyst layer have the inherent tendency to agglomerate into bigger particles to reduce their high surface energy [91,92]. Carbon oxidation or corrosion weakens the attachment of Pt particles to the carbon surface and eventually leads to structural collapse and detachment from the carbon support, resulting in the agglomeration and/or dissolution of Pt particles into the electrolyte without redeposition. Moreover, Pt may be transported through the electrolyte and/or through the ionomer after being detached, causing a reduction in electrolyte conductivity [93]. Therefore, carbon oxidation promoted by high cathode potential during the startup and shutdown processes is the main cause of catalyst degradation in the cathode of the fuel cell [43].

3.2.4. *Agglomeration and/or dissolution of Pt particles*

The degradation mechanisms for Pt catalysts include the following [32,48]:

- Pt particle agglomeration and particle growth.
- Pt loss and redistribution.
- Poisonous effects aroused by contaminants.

Once oxidation of the catalyst support happens during the startup and shutdown processes, the degradation of Pt particles follows the first two mechanisms. However, there is no consensus on the dominance of these two mechanisms. Some researchers have investigated the degradation process of a Pt catalyst during extended operation under OCV [92,93]. The results indicated that Pt particles dissolved in the ionomer and then grew to larger particles. Other researchers suggested that Pt particles would detach from the oxidized carbon support and dissolve in the electrolyte [94,95].

Cross-sectional scanning electron microscopy (SEM) and transmission electron microscopy (TEM) have often been used to characterize Pt/C catalysts subjected to frequent startup and shutdown cycles. Yi reported [43] that the thicknesses of the catalyst layers in the anode and cathode of fresh MEAs were 9.81 and 9.60 μm, which decreased to 7.02 and 2.47 μm, respectively, after 1500 frequent startup and shutdown cycles for an open-ended fuel cell (see Fig. 9). Ettingshausen et al. [45] observed the growth of Pt particles by using TEM and high resolution TEM to analyze a Pt/C catalyst that had experienced start/stop cycles and high cathode potential. After the start/stop cycles, the relative number of particles with a diameter ≤2.5 nm declined from 57.20% in a fresh MEA to 1.92%. Cho et al. combined the results of cross-sectional SEM and TEM to evaluate Pt/C degradation [33,34,36,38,39,45,59].

Apparently, a support material that is more stable than the current carbon support for PEMFC catalysts is desirable to alleviate the degradation caused by the startup and shutdown processes. But if the current catalyst-support technology has to be employed, there is an urgent need to apply effective system strategies for startup and shutdown to mitigate oxidation of the carbon support under high cathode potential.

4. Mitigation strategies

Many journal publications and patents have focused on the development of strategies to mitigate the performance decay caused by startup and shutdown. The strategies can be classified into two major categories:

- Material improvement for more stable catalyst supports.
- System mitigation strategies for conventional carbon-black supports.

4.1. Alternative catalyst supports

Replacing conventional carbon supports with corrosion-resistant materials has been one important mitigation strategy. Yu et al. [66] reported that using graphitized carbon as a support yielded a 5 times lower degradation rate than a conventional carbon support after 1000 startup/shutdown cycles. Owenjan et al. [30] also reported a 25% reduction in the startup/shutdown degradation rate at 1.2 A cm^{-2} with the implementation of a graphitized carbon in the microporous layers (MPL). They explained that the use of graphitized carbon resulted in a reduced mass transport limitation of the gas diffusion layer, in comparison with the mass transport limitation enhanced by conventional carbon oxidation at the MPL/electrode interface. In addition to graphitized carbon, other carbon materials, such as carbon nanotubes or carbon nanofibers [96–99], and carbon aerogel and xerogel [100–102], have also been considered as catalyst supports because of their more stable electrochemical behaviors [32]. However, the high cost of synthesizing these carbon materials increased the burden on the commercial development of PEMFCs. In addition to carbon-type supports, many non-carbon supports [63,103–108], such as substoichiometric titanium oxide [107], tungsten carbide [104], and indium tin oxide [105], have been investigated to replace the conventional carbon supports and achieve greater stability during long-term tests.

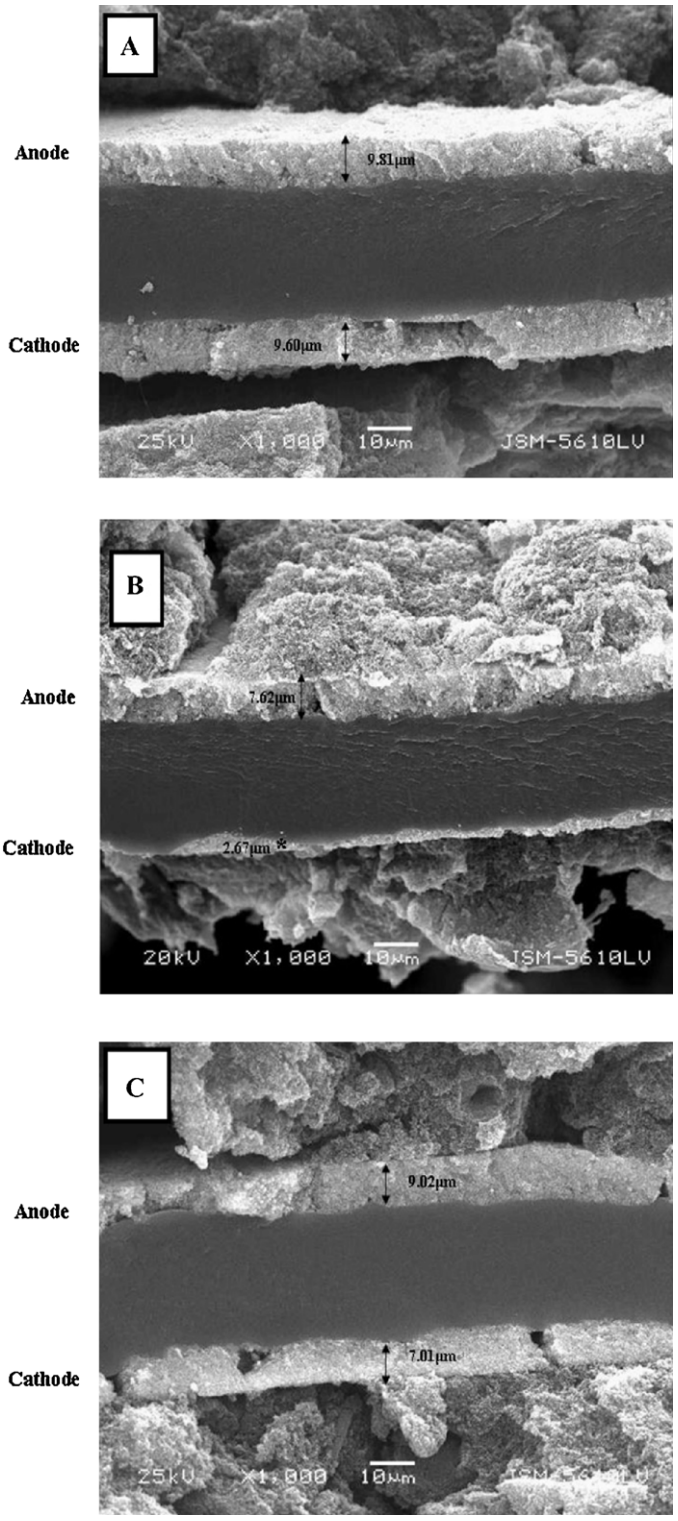

Fig. 9. Cross-sectional SEM images: (A) fresh MEA without startup–shutdown cycles; (B) MEA in open-ended cell after 1500 cycles; (C) MEA in closed cell after 1500 cycles.
Reprinted from Ref. [43] with permission.

Ioroi et al. [107] tested a single cell using a Pt/Ti_4O_7 cathode at 300 mA cm^{-2} for more than 350 h with fully humidified H_2/O_2. Stable voltage was observed throughout operation, demonstrating that Pt/Ti_4O_7 was a possible oxidation-resistant catalyst material for a PEMFC cathode. However, no reports have been published on durability tests of PEMFCs under startup and shutdown cycles using non-carbon supports.

As a result, system strategies seem more practical at the present time, when conventional carbon is being used as a catalyst support.

4.2. System strategies

As discussed in previous sections, the hydrogen/air interface causing reversed current and high cathode potential is the root cause for PEMFC degradation during startup and shutdown. All the reported or patented system strategies were developed to prevent a hydrogen/air interface at the anode and eliminate high potential at the cathode during startup and shutdown.

UTC, General Motors Corporation (GM), and other automotive companies such as Ford, Toyota, Nissan, and Daimler Chrysler have been researching system strategies for the startup and shutdown processes. Table 3 lists important patents on system strategies, including:

- Gas purge to anode before startup and after shutdown.
- Auxiliary load applied to consume residual oxygen at the cathode with potential control.
- Exhaust gas recycle as purging gas or reaction gas.
- Electronic short to eliminate high potential at the cathode.

4.2.1. Gas purge

Gas purging is an effective way to prevent a hydrogen/air interface at the anode. It can also minimize the time that an interface exists.

For the shutdown process of fuel cells, Margiott [115] and Reiser [116] at UTC have proposed the following procedure with air purging: supplying the air through the blower into the anode to dispel the residual hydrogen at the anode, after disconnecting the primary load and stopping the hydrogen supply. Reiser's long-term durability test [120] revealed an average voltage loss of 0.2 V without air purging after about 250 startup and shutdown cycles; however, the performance degradation was not so severe, with only about 0.055 V voltage loss after nearly 500 cycles with air purging (see Table 4). Yu and Wagner at General Motors Company [128–130] reported that air purging during the shutdown process was an effective method to prevent performance degradation in fuel cells. However, they proposed that it was more effective to employ the air purge until the temperature of the stack was reduced below a predetermined temperature.

With regard to the startup process, Balliet [119] and Reiser [120] invented a safety strategy that consisted of a startup system and method for a fuel cell power plant using a purging of the cathode flow field with a hydrogen-rich, reducing fluid fuel to minimize corrosion of the cathode electrode. Their strategy included the following steps: (1) purging the cathode flow field with the reducing fluid fuel; (2) directing the reducing fluid fuel to flow through an anode flow field; (3) terminating the flow of the fluid fuel through the cathode flow field and directing an oxygen-containing oxidant to flow through the cathode flow field; and (4) connecting a primary load to the fuel cell. In addition, General Motors also patented their invention of a startup process with gas purging, which included introducing hydrogen gas into the anode and the cathode to consume/purge oxygen in both [127].

It should be noted that in implementing the above mentioned system strategies, the blowers and other devices used to move the gases through the system should be properly selected to achieve the desired speed for gas displacement to occur in less than about 1.0 s, and preferably less than 0.2 s, to minimize the time that the hydrogen/air interface exists.

Nitrogen is a safe and inert gas that has been widely used as a purgative for fuel cells, but it is not easily made available in real fuel cell operations. To have nitrogen as a purging gas for startup and shutdown, Ford Motor Company has invented a purging system with a separator that removes oxygen from the exhaust gas at the cathode. After several cycles of cathode exhaust gas, a reformate gas with a high nitrogen concentration and low oxygen concentration can be used as the purge gas [139]. Thampan invented a strategy that used a membrane-based humidifier to provide a N_2-rich exhaust as the purging gas [151]. The membrane-based humidifier was used to transfer moisture from a moisture-laden exhaust stream to the dry air feed, and was also used in a shutdown mode in which the membrane-based humidifier was implemented to permeate moisture and oxygen from the moisture-laden exhaust stream, thereby providing nitrogen-rich gas. The same method was also patented by Scotto [154,155].

4.2.2. Auxiliary load with potential control

Gas purging can prevent a hydrogen/air interface during the startup and shutdown processes. However, it cannot completely dispel residual gas present in the flow field of fuel cells, such as in the gas diffusion layer or the catalyst layer. Another effective way to dispel residual gas is to introduce an auxiliary load (also called a dummy load). Kim et al. [36] have investigated how applying a dummy load affects fuel cell degradation. Their results indicated that application of a dummy load during the startup procedure significantly reduced performance decay and loss of electrochemically active surface area, and increased charge-transfer resistance, which resulted in a dramatic improvement in durability. In Condit's [112] and Balliet's [113] invention, a dummy load was applied to prevent cell reversal by consuming the air at the cathode during the shutdown process. Yu [129] applied an auxiliary load to consume the oxygen at the cathode, leaving nitrogen and hydrogen in the cathode and anode, respectively, during the shutdown process.

An auxiliary load has always been used in the company of an anode exhaust recycle loop. Yang proposed a startup procedure for a fuel cell system having an anode exhaust recycle loop [121]. First, the auxiliary load was connected across the cell to reduce the cell voltage. Then the limited hydrogen fuel from the anode exhaust, through a recycle loop, was provided to the anode. The added fuel reacted with the oxygen that remained in the recirculation gases until virtually no oxygen remained within the recycle loop. Finally, fuel and air could be supplied at the normal operating flow rates into the anode and cathode, respectively, after the auxiliary load was shut off. Fig. 10 shows the application of a dummy load during fuel introduction at startup [87]. The losses without a dummy load were severe, and the performance decreased by $\sim$100 $\mu V\,cycle^{-1}$. With a dummy load to control the cell voltage, performance decay was reduced to approximately 4 $\mu V\,cycle^{-1}$. Yang et al. patented a similar strategy that applied an auxiliary load with the anode recycle loop, and could be used in the shutdown process to reduce the cell potential [110,121].

Chan et al. at Hyundai Motor [149] have designed an apparatus for effectively preventing carbon corrosion from occurring at the cathode of a fuel cell. In this strategy, to completely exhaust the residual oxygen at the cathode after the fuel cell was shut down, a pressure sensor and an air discharge solenoid valve were installed in the air discharge pipe to detect the air pressure in the fuel cell and control the air supply. Under the function of the pressure sensor and the solenoid valve, as the residual oxygen at the cathode was completely consumed, the solenoid valve received the closing signal and the dummy load was disconnected to avoid a negative voltage in the fuel cell.

Table 3
Summary of patents on system strategies for startup and shutdown processes.

Inventors	Year	System strategy	Reference
UTC	2000	Making the fuel cell system inert by coolant flooding during shutdown	[109]
	2002	Shutting down the fuel cell system using an anode exhaust recycle loop	[110]
	2003		[111]
	2003	Shutting down fuel cells with an auxiliary load to consume the oxygen	[112]
	2004	Shutting down fuel cells with an auxiliary load to consume the oxygen	[113]
	2004	Fuel purge of cascaded fuel cell stacks	[114]
	2004	Shutting down fuel cells with an air purge into the anode	[115]
	2005		[116]
	2005	Cascaded anode inlet manifold design	[117]
	2005	Reducing cathode potential for the MEA with an electronic short	[118]
	2005	Starting up fuel cells with fuel purge into the cathode	[119,120]
	2006	Starting up a fuel cell system using an anode exhaust recycle loop	[121]
	2006	Using a hydrogen reservoir to receive and store hydrogen during fuel cell operation, and to release hydrogen whenever the fuel cell is shut down	[122]
	2011	Preventing air intrusion into hydrogen during shutdown	[123]
GM Motors Corporation	2005	Shutting down and starting up with a stoichiometric staged combustor	[124]
	2005	Shutdown and startup with a cathode recycle loop	[125,126]
	2006	Shutdown and startup with a hydrogen purge	[127]
	2006	Shutting down the fuel cell system using an air purge in low temperature	[128]
	2008	Shutting down with an auxiliary load to make nitrogen and hydrogen in the cathode and anode	[129]
	2008	Shutting down the fuel cell system using an air purge	[130]
	2008	Hydrogen purge into the cathode for operating a fuel cell stack	[131]
	2008	Special electrode design for reducing electrode degradation	[132]
	2009	Special electrode design containing oxygen evolution reaction catalysts	[133]
	2011	Fuel cell operating methods for oxygen depletion at shutdown	[134]
Plug Power	2007	Gas purge for startup and shutdown	[135]
Ballard Power Systems	2005	New catalyst design to improve voltage reversal tolerance	[136,137]
	2006		
	2007	Recirculating the oxidant with an anode purge path	[138]
Ford Motor Company	2009	Purging system with a separator that removes oxygen from the exhaust gas at the cathode	[139]
Nissan Motor	2009	Fuel cell system with voltage sensor and accurate gas-supply control	[140–142]
	2006		
	2005		
Daimler Chrysler	2011	A selectively conducting component is incorporated in electrical series with the anode	[143,144]
	2009	components in the fuel cell	
Honda Motor	2010	A fuel cell system that includes an oxidant gas supply apparatus and a fuel gas supplier	[145]
Toyota Motor	2009	The restriction on the output of the fuel cell is lifted, and the output of the fuel cell is	[146–148]
	2008	controlled according to the requested output	
Hyundai Motor	2008	Apparatus for preventing carbon corrosion at the cathode in the fuel cell	[149]
		Anode side hydrogen/oxygen interface formation inhibition structure	[150]
Others	2010	Membrane-based humidifier to provide a N_2-rich exhaust for purging gas	[151]
	2011	Shutting down with cathode gas recycle	[152]
	2010	Detecting the anode gas amount	[153]
	2011	Generating a gas that may be used for fuel cell startup and shutdown	[154,155]
	2008	Startup and shutdown with an electrical shorting device for individual cell shorting	[156]
	2006	Electrically connecting output terminals coupled to the fuel cell with a battery after shutting down to consume the oxygen and fuel gas	[157]
	2005	Starting up with a fuel purge	[158]
	2010	Using chemical shorting during startup and shutdown	[159]
	2008	Detecting air pressure to prevent a hydrogen/air interface	[160]
	2002	Safety process and device with the anode gas cycle	[161]
	2007	Shutting down with storing fuel in the anode and cathode chambers	[162]
	2009	System and method for starting up and shutting down	[163]

Another way of applying an auxiliary load is to use an electronic short of the fuel cell. Bekkedahl [118] invented a specially designed fuel cell stack with a permanent shunt, a diode, and a strip of conductive carbon cloth or black. The removable shunt could be rotated into and out of contact with the fuel cell anodes and cathodes to make an internal auxiliary load. Ramani [159] and Miller [156] also applied chemical shorting during the startup and shutdown processes.

4.2.3. Other system strategies

In addition to gas purging and auxiliary load strategies, other system strategies have been developed to enhance the durability of PEMFCs during startup and shutdown. They include novel catalyst design to improve the catalyst's tolerance to voltage reversal [136], unique electrode design to reduce electrode degradation under startup and shutdown [132], use of an electrode that contains oxygen evolution reaction catalysts to prevent current reversal [133], and application of a cascade fuel inlet manifold [114,117] to achieve better hydrogen distribution in the flow filed.

Some Japanese companies, such as Toyota Motor [146–148], Seiko Instruments [164], Nissan Motor [140–142], Fuji Electric [165], and Daihatsu Motor [166], have proposed their own PEMFC systems with voltage sensors and accurate gas-supply control

Table 4
Summary of system strategies, with durability test results for startup and shutdown processes.

Inventors	System strategies	Durability test result		Reference
Reiser et al.	Uncontrolled startup and shutdown	Average voltage loss: 0.195 V after 250 cycles		[116,120]
	Startup and shutdown with H_2 purge into the cathode, with an auxiliary load	Average voltage loss: 0.055 V after 300 cycles		
	N_2 purge during the startup and shutdown cycles	Average voltage loss: 0.04 V after 1550 cycles		
Condit et al.	Shutdown with auxiliary load and H_2 recycle loop; startup with auxiliary load and N_2 purge	Average voltage decreased from 0.760 V to 0.695 V in 576 cycles at 400 mA cm^{-2}		[112]
	Shutdown with auxiliary load and H_2 recycle loop; startup with H_2 and N_2 stored at the anode and cathode	Average voltage recovered from 0.695 V to 0.755 V after 2315 cycles at 400 mA cm^{-2}		
Bekkedahl et al.	Reducing fuel cell cathode potential with electronic short	Cell voltage decayed much less after 230–256 startup and shutdown cycles at 108 mA cm^{-2} and 325 mA cm^{-2}		[118]
Yu et al.	Shutting down fuel cell system by using air purge at low cell temperature (after 40 cycles)	30 °C	Voltage loss: 0.0142 V at 200 mA cm^{-2} Voltage loss: 0.0322 V at 800 mA cm^{-2}	[128,130]
		50 °C	Voltage loss: 0.0327 V at 200 mA cm^{-2} Voltage loss: 0.1486 V at 800 mA cm^{-2}	
		80 °C	Voltage loss: 0.1937 V at 200 mA cm^{-2} Voltage loss: 0.4092 V at 800 mA cm^{-2}	
Yu et al.	Shutdown and startup with H_2 purge	Cell voltage decreased from 0.79 V to 0.78 V after 200 cycles		[127]
Tang et al.	H_2 purge for startup and shutdown	Performance with H_2-purge protection is better than with N_2-purge protection after startup and shutdown cycles		[135]
Thampan et al.	Membrane-based humidifier to provide a N_2-rich exhaust for purging gas	No N_2 purge	Cell voltage decreased from 0.65 V to 0.47 V at 600 mA cm^{-2}	[151]
		With N_2 purge	Cell voltage decreased from 0.65 V to 0.55 V at 600 mA cm^{-2}	
Ramani et al.	Chemically shorted MEA with H_2 and air bleed purge	Average voltage decreased from 0.69 V to 0.50 V at 600 mA cm^{-2} after 350 startup and shutdown cycles		[159]
Paik et al.	Purge system with a separator to remove oxygen from the exhaust gas at the cathode	Air/H_2 cycling at anode	Voltage decreased from 0.78 V to 0.25 V at 600 mA cm^{-2} after 500 cycles	[139]
		N_2 purge at anode	Voltage decreased from 0.39 V to 0.25 V at 600 mA cm^{-2} after 639 cycles	
		5% O_2 in nitrogen purge at anode	Voltage decreased from 0.6 V to 0.44 V at 1000 mA cm^{-2} after 500 cycles	
		10% O_2 in nitrogen purge at anode	Voltage decreased from 0.7 V to 0.4 V at 500 mA cm^{-2} after 40 cycles	

systems to achieve a desirable durability during the startup and shutdown processes.

4.2.4. Summary of system strategies

As shown in Table 4, recent patents have reported several durability tests conducted with different system strategies under startup and shutdown cycles. The performance decay was greatly mitigated by various strategies, among which the most effective was the combination of hydrogen purging, application of an auxiliary load, and use of a voltage control device to prevent voltage reversal. All the system strategies listed in Table 4 are based on the following two principles:

- Minimizing the time that the hydrogen/air interface exists, such as by using fuel purging during the startup and shutdown processes, and producing N_2-rich gas with a special system design.
- Reducing the potentials during the startup and shutdown processes, such as by applying an external auxiliary load and by creating an internal short in the fuel cells.

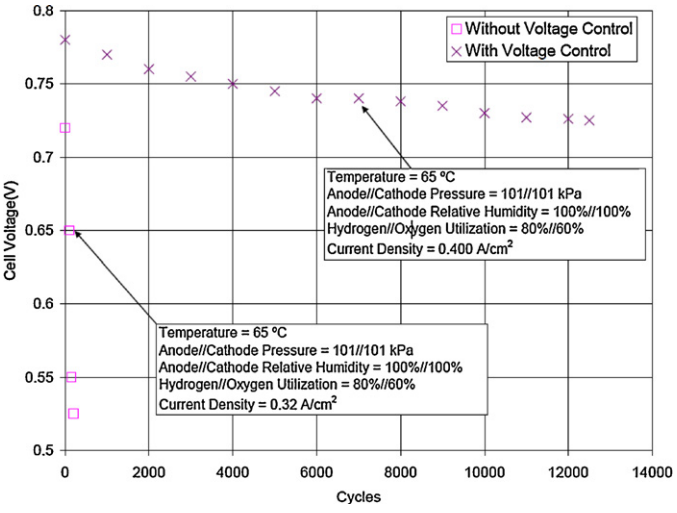

Fig. 10. Effect of voltage control during fuel introduction on performance loss. Reprinted with permission from Ref. [87]. Copyright 2006, The Electrochemical Society).

In comparison with materials improvement by using graphitized carbon or non-carbon supports, system strategies are relatively simple and cheap to implement in real fuel cell engines.

It is urgently necessary to set up relevant procedures and devices to meet the durability requirements of PEMFCs.

5. Concluding remarks

Performance degradation during startup and shutdown is an important issue that affects the durability and lifetime of PEMFCs. This review paper has surveyed and analyzed the durability tests, degradation mechanisms, and system strategies for the startup and shutdown processes.

The high potential at the cathode, introduced by the hydrogen/air interface at the anode, is the major cause of performance degradation of PEMFCs. A great deal of work has been done to develop alternative novel catalyst supports and system strategies to mitigate catalyst degradation. Currently, several strategies have greatly enhanced the durability of PEMFCs during the startup and

shutdown cycles, such as applying a hydrogen purge and an auxiliary load.

Further work is needed to apply these effective strategies in more fuel cell systems. By combining system strategies with novel catalyst supports that have better corrosion resistance, the performance degradation caused by the startup and shutdown processes can be avoided to achieve long lifetimes that can meet the durability requirements for PEMFCs.

Acknowledgements

Yi Yu thanks the China Scholarship Council and the National Research Council Canada (NRC) for financial support through the NRC-MOE Research and Post-doctoral Fellowship Program.

References

[1] W. Vielstich, H. Yokokawa, H.A. Gasteiger, Handbook of Fuel Cells: Fundamentals, Technology, and Applications. Advances in Electrocatalysis, Materials, Diagnostics and Durability, Part 1, Wiley, 2009.
[2] R. Borup, J. Meyers, B. Pivovar, Y.S. Kim, R. Mukundan, N. Garland, D. Myers, M. Wilson, F. Garzon, D. Wood, Chemical Reviews 107 (2007) 3904–3951.
[3] Hydrogen, Fuel Cells & Infrastructure Technologies Program Multi-Year Research, Development and Demonstration Plan, August 2006, http://www1.eere.energy.gov/hydrogenandfuelcells/mypp.
[4] T. Payne, Fuel Cells Durability & Performances, The Knowledge Press Inc., US Brookline, 2009.
[5] P. Pei, Q. Chang, T. Tang, International Journal of Hydrogen Energy 33 (2008) 3829–3836.
[6] J. Wu, X.Z. Yuan, J.J. Martin, H. Wang, J. Zhang, J. Shen, S. Wu, W. Merida, Journal of Power Sources 184 (2008) 104–119.
[7] T.R. Ralph, Platinum Metals Review 41 (1997) 102–113.
[8] J. St-Pierre, D.P. Wilkinson, S. Knights, M.L. Bos, Journal of New Materials for Electrochemical Systems 3 (2000) 99–106.
[9] K. Washington, Proceedings of Fuel Cell Seminar 2000, 2000, pp. 468–472.
[10] S.Y. Ahn, S.J. Shin, H.Y. Ha, S.A. Hong, Y.C. Lee, T.W. Lim, I.H. Oh, Journal of Power Sources 106 (2002) 295–303.
[11] M.W. Fowler, R.F. Mann, J.C. Amphlett, B.A. Peppley, P.R. Roberge, Journal of Power Sources 106 (2002) 274–283.
[12] J. St-Pierre, N. Jia, Journal of New Materials for Electrochemical Systems 5 (2002) 263–271.
[13] O. Yamazaki, M. Echigo, T. Tabata, Proceedings of Fuel Cell Seminar 2002, 2002, pp. 105–108.
[14] X. Cheng, L. Chen, C. Peng, Z. Chen, Y. Zhang, Q. Fan, Journal of the Electrochemical Society 151 (2004) A48–A52.
[15] J. Scholta, N. Berg, P. Wilde, L. Jörissen, J. Garche, Journal of Power Sources 127 (2004) 206–212.
[16] S.J.C. Cleghorn, D.K. Mayfield, D.A. Moore, J.C. Moore, G. Rusch, T.W. Sherman, N.T. Sisofo, U. Beuscher, Journal of Power Sources 158 (2006) 446–454.
[17] E. Endoh, H. Kawazoe, S.S. Honmura, Proceedings of Fuel Cell Seminar 2006, 2006, pp. 284–287.
[18] C. Sishtla, G. Koncar, R. Platon, S. Gamburzev, A.J. Appleby, O.A. Velev, Journal of Power Sources 71 (1998) 249–255.
[19] T. Isono, S. Suzuki, M. Kaneko, Y. Akiyama, Y. Miyake, I. Yonezu, Journal of Power Sources 86 (2000) 269–273.
[20] H. Meada, A. Yoshimura, H. Fukumoto, Proceedings of the 2000 Fuel Cell Seminar, 2000, pp. 379–400.
[21] T. Nakayama, Proceedings of the 2000 Fuel Cell Seminar, 2000, pp. 391–394.
[22] S. Sakamoto, A. Fuju, K. Shindo, S. Yoshida, K. Nakato, N. Nishizawa, Proceedings of Fuel Cell Seminar 2000, 2000, pp. 85–94.
[23] M. Fowler, J.C. Amphlett, R.F. Mann, B.A. Peppley, P.R. Roberge, Journal of New Materials for Electrochemical Systems 5 (2002) 255–262.
[24] E. Cho, J.J. Ko, H.Y. Ha, S.A. Hong, K.Y. Lee, T.W. Lim, I.H. Oh, Journal of the Electrochemical Society 151 (2004) A661–A665.
[25] M. Oszcipok, D. Riemann, U. Kronenwett, M. Kreideweis, M. Zedda, Journal of Power Sources 145 (2005) 407–415.
[26] J. Xie, D.L. Wood Iii, D.M. Wayne, T.A. Zawodzinski, P. Atanassov, R.L. Borup, Journal of the Electrochemical Society 152 (2005) A104–A113.
[27] J. Yu, T. Matsuura, Y. Yoshikawa, M.N. Islam, M. Hori, Electrochemical and Solid-State Letters 8 (2005) A156–A158.
[28] B. Du, R. Pollard, J. Elter, Proceedings of Fuel Cell Seminar 2006, 2006, pp. 61–64.
[29] H. Xu, M. Wu, Y. Liu, V. Mittal, R. Vieth, H.R. Kunz, L.J. Bonville, J.M. Fenton, ECS Transactions 3 (2006) 561–568.
[30] J.E. Owejan, P.T. Yu, R. Makharia, ECS Transactions 11 (2007) 1049–1057.
[31] W. Schmittinger, A. Vahidi, Journal of Power Sources 180 (2008) 1–14.
[32] S. Zhang, X.Z. Yuan, J.N.C. Hin, H. Wang, K.A. Friedrich, M. Schulze, Journal of Power Sources 194 (2009) 588–600.
[33] Y.Y. Jo, E. Cho, J.H. Kim, T.H. Lim, I.H. Oh, S.K. Kim, H.J. Kim, J.H. Jang, Journal of Power Sources 196 (2011) 9906–9915.
[34] Y.Y. Jo, E.A. Cho, J.H. Kim, T.H. Lim, I.H. Oh, J.H. Jang, H.J. Kim, International Journal of Hydrogen Energy 35 (2010) 13118–13124.
[35] H.J. Kim, S.J. Lim, J.W. Lee, I.G. Min, S.Y. Lee, E.A. Cho, I.H. Oh, J.H. Lee, S.C. Oh, T.W. Lim, Journal of Power Sources 180 (2008) 814–820.
[36] J.H. Kim, E.A. Cho, J.H. Jang, H.J. Kim, T.H. Lim, I.H. Oh, J.J. Ko, S.C. Oh, Journal of the Electrochemical Society 156 (2009) B955–B961.
[37] J.H. Kim, E.A. Cho, J.H. Jang, H.J. Kim, T.H. Lim, I.H. Oh, J.J. Ko, S.C. Oh, Journal of the Electrochemical Society 157 (2010) B104–B112.
[38] J.H. Kim, Y. Yeon Jo, E.A. Cho, J.H. Jang, H.J. Kim, T.H. Lim, I.H. Oh, J.J. Ko, I.J. Son, Journal of the Electrochemical Society 157 (2010) B633–B642.
[39] S.Y. Lee, E. Cho, J.H. Lee, H.J. Kim, T.H. Lim, I.H. Oh, J. Won, Journal of the Electrochemical Society 154 (2007) B194–B200.
[40] Y. Takagi, Y. Takakuwa, ECS Transactions 3 (2006) 855–860.
[41] Y. Ishigami, K. Takada, H. Yano, J. Inukai, M. Uchida, Y. Nagumo, T. Hyakutake, H. Nishide, M. Watanabe, Journal of Power Sources 196 (2011) 3003–3008.
[42] H. Tang, Z. Qi, M. Ramani, J.F. Elter, Journal of Power Sources 158 (2006) 1306–1312.
[43] Y. Yu, Z. Tu, H. Zhang, Z. Zhan, M. Pan, Journal of Power Sources 196 (2011) 5077–5083.
[44] T.W. Patterson, R.M. Darling, Electrochemical and Solid-State Letters 9 (2006) A183–A185.
[45] F. Ettingshausen, J. Kleemann, A. Marcu, G. Toth, H. Fuess, C. Roth, Fuel Cells 11 (2011) 238–245.
[46] P. He, T.T.H. Cheng, R. Bashyam, A.P. Young, S. Knights, ECS Transactions 33 (2010) 1273–1279.
[47] C.A. Reiser, L. Bregoli, T.W. Patterson, J.S. Yi, J.D. Yang, M.L. Perry, T.D. Jarvi, Electrochemical and Solid-State Letters 8 (2005) A273–A276.
[48] N. Yousfi-Steiner, P. Moçotéguy, D. Candusso, D. Hissel, Journal of Power Sources 194 (2009) 130–145.
[49] D. Devilliers, É. Mahé, Cellules électrochimiques: Aspects thermodynamiques et cinétiques: Applications aux générateurs et aux électrolyseurs industriels 13 (2003) 31–40.
[50] W.R. Baumgartner, P. Parz, S.D. Fraser, E. Wallnöfer, V. Hacker, Journal of Power Sources 182 (2008) 413–421.
[51] J. Ihonen, F. Jaouen, G. Lindbergh, A. Lundblad, G. Sundholm, Journal of the Electrochemical Society 149 (2002) A448–A454.
[52] M. Kunimatsu, H. Qiao, T. Okada, Journal of the Electrochemical Society 152 (2005) E161–E166.
[53] G. Li, P.G. Pickup, Electrochimica Acta 49 (2004) 4119–4126.
[54] G. Li, P.G. Pickup, Electrochemical and Solid-State Letters 9 (2006) A249–A251.
[55] Z. Siroma, R. Kakitsubo, N. Fujiwara, T. Ioroi, S.I. Yamazaki, K. Yasuda, Journal of Power Sources 156 (2006) 284–287.
[56] Q. Shen, M. Hou, D. Liang, Z. Zhou, X. Li, Z. Shao, B. Yi, Journal of Power Sources 189 (2009) 1114–1119.
[57] R.A. Sidik, Journal of Solid State Electrochemistry 13 (2009) 1123–1126.
[58] J.H. Ohs, U. Sauter, S. Maass, D. Stolten, Journal of Power Sources 196 (2011) 255–263.
[59] J. Kim, J. Lee, Y. Tak, Journal of Power Sources 192 (2009) 674–678.
[60] D. Liang, Q. Shen, M. Hou, Z. Shao, B. Yi, Journal of Power Sources 194 (2009) 847–853.
[61] M. Dou, M. Hou, D. Liang, Q. Shen, H. Zhang, W. Lu, Z. Shao, B. Yi, Journal of Power Sources 196 (2011) 2759–2762.
[62] D. Liang, M. Dou, M. Hou, Q. Shen, Z. Shao, B. Yi, Journal of Power Sources 196 (2011) 5595–5598.
[63] S. Maass, F. Finsterwalder, G. Frank, R. Hartmann, C. Merten, Journal of Power Sources 176 (2008) 444–451.
[64] S. Von Dahlen, G.G. Scherer, A. Wokaun, I.A. Schneider, ECS Transactions 33 (2010) 1365–1374.
[65] I.A. Schneider, S. Von Dahlen, Electrochemical and Solid-State Letters 14 (2011) B30–B33.
[66] P.T. Yu, W. Gu, R. Makharia, F.T. Wagner, H.A. Gasteiger, ECS Transactions 3 (2006) 797–809.
[67] J.P. Meyers, R.M. Darling, Journal of the Electrochemical Society 153 (2006) A1432–A1442.
[68] N. Takeuchi, T.F. Fuller, Journal of the Electrochemical Society 157 (2010) B135–B140.
[69] J. Hu, P.C. Sui, S. Kumar, N. Djilali, ECS Transactions 11 (2007) 1031–1039.
[70] Z. Qi, H. Tang, Q. Guo, B. Du, Journal of Power Sources 161 (2006) 864–871.
[71] W. Gu, R.N. Carter, P.T. Yu, H.A. Gasteiger, ECS Transactions 11 (2007) 963–973.
[72] X. Wang, K. Tajiri, R.K. Ahluwalia, Journal of Power Sources 195 (2010) 6680–6687.
[73] J. Hu, P.C. Sui, S. Kumar, N. Djilali, Electrochimica Acta 54 (2009) 5583–5592.
[74] A.B. Ofstad, J.R. Davey, S. Sunde, R.L. Borup, ECS Transactions 16 (2008) 1301–1311.
[75] K.D. Baik, M.S. Kim, International Journal of Hydrogen Energy 36 (2011) 732–739.
[76] J. Crank, The Mathematics of Diffusion, Clarendon Press, Oxford, 1970.
[77] H. Sun, G. Zhang, L.J. Guo, H. Liu, Journal of Power Sources 158 (2006) 326–332.
[78] H. Sun, G. Zhang, L.J. Guo, S. Dehua, H. Liu, Journal of Power Sources 168 (2007) 400–407.
[79] T. Hottinen, M. Noponen, T. Mennola, O. Himanen, M. Mikkola, P. Lund, Journal of Applied Electrochemistry 33 (2003) 265–271.
[80] D. Natarajan, T. Van Nguyen, AIChE Journal 51 (2005) 2587–2598.

[81] Z. Liu, Z. Mao, B. Wu, L. Wang, V.M. Schmidt, Journal of Power Sources 141 (2005) 205–210.
[82] Z. Liu, L. Yang, Z. Mao, W. Zhuge, Y. Zhang, L. Wang, Journal of Power Sources 157 (2006) 166–176.
[83] F. Cocuret, Ingénierie des Procédes Electrochimiqucs (2003).
[84] M. Carmo, V.A. Paganin, J.M. Rosolen, E.R. Gonzalez, Journal of Power Sources 142 (2005) 169–176.
[85] E.P. Ambrosio, C. Francia, C. Gerbaldi, N. Penazzi, P. Spinelli, M. Manzoli, G. Ghiotti, Journal of Applied Electrochemistry 38 (2008) 1019–1027.
[86] E. Antolini, Applied Catalysis B: Environmental 88 (2009) 1–24.
[87] M.L. Perry, T.W. Patterson, C. Reiser, ECS Transactions 3 (2006) 783–795.
[88] Y. Shao, G. Yin, Y. Gao, Journal of Power Sources 171 (2007) 558–566.
[89] L.M. Roen, C.H. Paik, T.D. Jarvi, Electrochemical and Solid-State Letters 7 (2004) A19–A22.
[90] J. Willsau, J. Heitbaum, Journal of Electroanalytical Chemistry 161 (1984) 93–101.
[91] T.R. Ralph, S. Hudson, D.P. Wilkinson, ECS Transactions 1 (2005) 67–84.
[92] P.J. Ferreira, G.J. La O, Y. Shao-Horn, D. Morgan, R. Makharia, S. Kocha, H.A. Gasteiger, Journal of the Electrochemical Society 152 (2005) A2256–A2271.
[93] A.V. Virkar, Y. Zhou, Journal of the Electrochemical Society 154 (2007) B540–B547.
[94] K.L. More, R. Borup, K.S. Reeves, ECS Transactions 3 (2006) 717–733.
[95] K.J.J. Mayrhofer, J.C. Meier, S.J. Ashton, G.K.H. Wiberg, F. Kraus, M. Hanzlik, M. Arenz, Electrochemistry Communications 10 (2008) 1144–1147.
[96] X. Wang, W. Li, Z. Chen, M. Waje, Y. Yan, Journal of Power Sources 158 (2006) 154–159.
[97] M.M. Waje, W. Li, Z. Chen, Y. Yan, ECS Transactions 3 (2006) 677–683.
[98] Y. Shao, G. Yin, Y. Gao, P. Shi, Journal of the Electrochemical Society 153 (2006) A1093–A1097.
[99] K. Lee, J. Zhang, H. Wang, D.P. Wilkinson, Journal of Applied Electrochemistry 36 (2006) 507–522.
[100] A. Smirnova, X. Dong, H. Hara, N. Sammes, Journal of Fuel Cell Science and Technology 3 (2006) 477–481.
[101] N. Job, J. Marie, S. Lambert, S. Berthon-Fabry, P. Achard, Energy Conversion and Management 49 (2008) 2461–2470.
[102] C.D. Saquing, D. Kang, M. Aindow, C. Erkey, Microporous and Mesoporous Materials 80 (2005) 11–23.
[103] H. Chhina, S. Campbell, O. Kesler, Journal of the Electrochemical Society 154 (2007) B533–B539.
[104] H. Chhina, S. Campbell, O. Kesler, Journal of Power Sources 179 (2008) 50–59.
[105] H. Chhina, S. Campbell, O. Kesler, Journal of Power Sources 161 (2006) 893–900.
[106] N. Rajalakshmi, H. Ryu, M.M. Shaijumon, S. Ramaprabhu, Journal of Power Sources 140 (2005) 250–257.
[107] T. Ioroi, H. Senoh, S.I. Yamazaki, Z. Siroma, N. Fujiwara, K. Yasuda, Journal of the Electrochemical Society 155 (2008) B321–B326.
[108] Y. Suzuki, A. Ishihara, S. Mitsushima, N. Kamiya, K.I. Ota, Electrochemical and Solid-State Letters 10 (2007) B105–B107.
[109] M.E. Gorman, U.S. Patent 6,127,057 (2000).
[110] D. Yang, M.M. Steinbugler, R.D. Sawyer, L.L.V. Dine, C.A. Reiser, U.S. Patent Appl. 0102443 A1 (2002).
[111] L.L.V. Dine, M.M. Steinbugler, C.A. Reiser, G.W. Scheffler, U.S. Patent 6,514,635 B2 (2003).
[112] D.A. Condit, R.D. Breault, U.S. Patent 6,635,370 (2003).
[113] R.J. Balliet, C.A. Reiser, U.S. Patent 6,835,479 (2004).
[114] M.L. Perry, P.R. Margiott, U.S. Patent 6,821,668 (2004).
[115] P.R. Margiott, C.W. Callahan, M.L. Perry, G.W. Scheffler, U.S. Patent 6,828,048 B2 (2004).
[116] C.A. Reiser, D. Yang, R.D. Sawyer, U.S. Patent 6,858,336 B2 (2005).
[117] J.H. Whiton, T.J. Anderson, R.J. Guthrie, U.S. Patent 6,924,056 B2 (2005).
[118] T.A. Bekkedahl, L.J. Bregoli, R.D. Breault, E.A. Dykeman, J.P. Meyers, T.W. Patterson, T. Skiba, C. Vargas, D. Yang, J.S. Yi, U.S. Patent 6,913,845 B2 (2005).
[119] R.J. Balliet, C.A. Reiser, T.W. Patterson, M.L. Perry, U.S. Patent 6,838,199 B2 (2005).
[120] C.A. Reiser, D. Yang, R.D. Sawyer, U.S. Patent 6,887,599 B2 (2005).
[121] D. Yang, M.M. Steinbugler, R.D. Sawyer, L.L.V. Dine, C.A. Reiser, U.S. Patent Appl. 0093879 A1 (2006).
[122] P.R. Margiott, F.R. Preli, G.W. Kulp, M.L. Perry, C.A. Resier, R.J. Balliet, U.S. Patent 6,984,464 B2 (2006).
[123] M.L. Perry, U.S. Patent Appl. 0223495 A1 (2011).
[124] W.H. Pettit, S.G. Goebel, U.S. Patent Appl. 0136304 A1 (2005).
[125] S.G. Goebel, U.S. Patent Appl. 0221148 A1 (2005).
[126] S.G. Goebel, U.S. Patent Appl. 0058859 A1 (2005).
[127] P.T. Yu, F.T. Wagner, U.S. Patent Appl. 0046106 A1 (2006).
[128] P.T. Yu, F.T. Wagner, U.S. Patent Appl. 0040150 A1 (2006).
[129] P.T. Yu, F.T. Wagner, G.W. Skala, B. Lakshmanan, J.P. Salvador, U.S. Patent Appl. 0145716 A1 (2008).
[130] P.T. Yu, F.T. Wagner, U.S. Patent Appl. 0003465 A1 (2008).
[131] P.T. Yu, U.S. Patent Appl. 0145717 A1 (2008).
[132] S. Swathirajan, B. Merzougui, P.T. Yu, U.S. Patent Appl. 0166599 A1 (2008).
[133] S.G. Yan, H.A. Gasteiger, P.T. Yu, W. Gu, J. Zhang, U.S. Patent Appl. 0068541 A1 (2009).
[134] T.W. Tighe, S.G. Goebel, G.M. Robb, A.B. Alp, B. Lakshmanan, J.N. Lovria, U.S. Patent Appl. 0143241 A1 (2011).
[135] H. Tang, Z. Qi, M. Ramani, K.M. Rush, L.F. Wong, N. Miklas, U.S. Patent Appl. 0154742 A1 (2007).
[136] S.D. Knights, D.P. Wilkinson, S.A. Campbell, J.L. Taylor, J.M. Gascoyne, T.R. Ralph, U.S. Patent 6,936,370 (2005).
[137] U.M. Limbeck, R. Holger, Patent CA2517627 (2006).
[138] B. Janusz, S. David, C. Anthony, H. Andrew, F. Richard, H. Steven, D. Michael, Patent WO2007044971 A1 (2007).
[139] C. Paik, J.A. Adams, G.S. Saloka, M.S. Sulek, U.S. Patent Appl. 0023040 A1 (2009).
[140] K. Mitsuhiro, S. Kazuo, M. Akira, S. Ryoichi, F. Takahiro, Y. Kenji, I. Takashi, T. Yasuhiro, K. Mitsunori, Patent JP2009181793 (2009).
[141] Y. Masanari, Patent JP2006155917 (2006).
[142] T. Yasuhiro, M. Shinichi, S. Hiromasa, Patent JP2005158557 (2005).
[143] B. Nicolae, B. Francine, F. Richard, H. Herwig, H. Yvonne, L. Andrew, P. Guy, R. Joy, Y.A. Shunwen, Patent WO2011076396 (2011).
[144] S. Joerg, W.T. Markus, Patent DE102007048317 (2009).
[145] S. Seiji, M. Hiroshi, U.S. Patent 2010081016 A1 (2010).
[146] X. Gang, Patent WO2009031444 (2009).
[147] S. Tsutomu, Patent WO2009010857 (2009).
[148] K. Hideaki, Patent WO2008146122 (2008).
[149] O.S. Chan, L.J. Hyun, Y.J. Jin, K. Jun, K.Y. Min, S.I. Jae, Patent DE102007057488 (2008).
[150] O.S. Chan, Patent KR100821771 (2008).
[151] T.M.K. Thampan, R. Benesch, U.S. Patent Appl. 0248044 A1 (2010).
[152] A. Knoop, U.S. Patent Appl. 0045368 A1 (2011).
[153] T. Kamiyama, N. Nakajima, T. Yamashiro, K. Miyata, U.S. Patent Appl. 0209793 A1 (2010).
[154] M.V. Scotto, D.P. Birmingham, C.L. DeBellis, M.A. Perna, G.C. Rush, U.S. Patent Appl. 0059376 A1 (2011).
[155] M.V. Scotto, D.P. Birmingham, C.L. DeBellis, M.A. Perna, G.C. Rush, U.S. Patent Appl. 0059377 A1 (2011).
[156] D.P. Miller, J.A. Rock, C.M. Marsiglio, U.S. Patent Appl. 0220294 A1 (2008).
[157] D.M. Suh, U.S. Patent Appl. 0228594 A1 (2006).
[158] G.W. Kulp, R.D. Breault, U.S. Patent Appl. 0142399 A1 (2005).
[159] M. Ramani, R.A. Dross, L. Mao, B. Du, U.S. Patent Appl. 0035098 A1 (2010).
[160] S.C. Oh, J.H. Lee, J.J. Yoon, J.J. Ko, Y.M. Kim, I.J. Son, U.S. Patent Appl. 0318099 A1 (2008).
[161] P. Charlat, U.S. Patent Appl. 0058167 A1 (2002).
[162] J.F. McElroy, D.T. Davis, M.D. Gasda, U.S. Patent Appl. 0154752 A1 (2007).
[163] U.M. Limbeck, M. Aberle, C.R. Louie, A.E. Nelson, U.S. Patent Appl. 0258256 A1 (2009).
[164] I. Noboru, I. Fumiharu, Y. Kazutaka, S. Takashi, O. Toru, Y. Takamasa, Patent JP2010055884 (2010).
[165] K. Shigemi, W. Takanori, Patent JP2009117238 (2009).
[166] Y. Tomonori, Y. Naoya, Patent JP2008243500 (2008).